Automatic and High-Precision Acoustic Emission-Based Structural Health Monitoring of Concrete Structures

SEYYEDMAALEK MOMENI, THOMAS SCHUMACHER, LINDSAY LINZER and BRICE LECAMPION

ABSTRACT

Acoustic emission (AE) monitoring is a useful technique to monitor the health of a structure continuously, helping to prevent potential failure. AE are elastic waves produced and emitted during fracture processes inside a material and are recorded by sensors. Using quantitative geophysics-based methods, the recorded signals can be processed to monitor and describe the spatio-temporal growth of fracture in brittle materials such as concrete in real-time. Because of the complex nature of the recorded elastic signals and the non-homogeneous medium condition of concrete, data are usually processed manually. Combined with the high processing cost of the large datasets collected, which may exceed Terabytes, this approach has not found many real-world applications. Thus, an automated methodology is needed that can reduce costs, while maintaining high-precision, for implementation in a structural health monitoring (SHM) scheme.

Here we discuss the application of a new automated and high-precision AE monitoring algorithm and software called SIMRGH [5,6] suitable for SHM of concrete structures. The core software has been developed for the laboratory-scale (in scale of centimeters) hydraulic fracture monitoring. It is up-scaled to the meters scale and works for heterogeneous media. The software works with various standard data formats and can handle trigger-based as well as continuous data. In this paper, we show some initial results of implementing the software for AE monitoring of two 4.88-meter-long concrete beams loaded in the laboratory and compare it with manually processed AE data. We were able to locate at least three up to 10 times more AE sources compared to when manual processing was used and with higher precision. If enough processing units are provided, the software can run in parallel and enable real-time SHM with excellent precision on crack geometry imaging. Future work will include implementing moment tensor inversion (MTI) to characterize AE source physics, providing valuable information for decision makers regarding the nature of the captured data.

Seyyedmaalek Momeni* and Brice Lecampion, Geo-Energy Laboratory, Gaznat chair on Geo-Energy, EPFL. Station 18, CH-1015, Lausanne, Switzerland
Thomas Schumacher, Civil & Environmental Engineering, Portland State University, Portland, OR 97201, Portland, USA
Lindsay Linzer, SRK Consulting Ltd, 265 Oxford Road, Illovo, Johannesburg, 2196, South Africa
*Corresponding author (email: seyyedmaalek.momeni@epfl.ch)

INTRODUCTION

Understanding how fractures originate and propagate in solid materials in various fields is crucial for two reasons. 1- Safety: i.e., to avoid failure in bridges, and, 2- productivity: i.e., in geothermal energy field where hydraulic fracturing is performed to enhance energy extraction from underground [1, 2].

AE monitoring is a key method for real-time measurement of the location and geometry of developing fractures. However, the commonly encountered heterogeneous solid media, which results in complexity in AE signals, obliges one to process them manually. Additionally, the size of the data, which is on the order of terabytes, grows linearly with the number of sensors being employed. Despite the benefits of AE monitoring, the aforementioned problems restrict its use and increase its expense. In fact, the majority of studies use fewer sensors to speed up processing. Furthermore, to only process significant AE events, a higher amplitude threshold is typically used during recording. However, these choices result in the loss of crucial information on fracture development and may cause users to miss ongoing fracture-related risks or report false alarms. On the other hand, precise localization of hundreds of AE sources by visual interpretation cannot be an optimal solution because of the possible mistakes happening during long processing.

All of the aforementioned problems emphasize the requirement for an automatic and reliable software that can perform fracture monitoring calculations with the highest level of accuracy. There have been several attempts in the literature to calculate the source localizations of elastic wave sources [3]. However, no automatic solution that is scalable and works in real-time can deliver accurate and reliable results to our knowledge. Deep learning algorithms fall under the previously described methodologies as well because they require reference data to properly train a neural network [4] and the desired precision usually may not be achieved.

For the first time, we demonstrate in this study the capabilities of a novel algorithm and software package called SIMORGH [5, 6], demonstrating the automatic processing of AE signals captured during various stages of loading of large-scale laboratory reinforced concrete beams. We show SIMORGH's performance on fracture monitoring data in both terms of speed and precision.

LABORATORY EXPERIMENTS

Specimens

Two large scale reinforced concrete beams with overall dimensions of $b \times h \times l$ = 305 mm × 610 mm × 4.88 m (12 in × 24 in × 16 ft) were tested in four-point bending configuration in the Structures Laboratory at the University of Delaware. Figure 1a, b shows the two tested beams, which were made of 31.0 MPa (4,500 psi) concrete and Grade 60 (f_y = 414 MPa) steel-reinforcing bars (rebars). The first beam was designed to fail in flexure at mid-span. A total of 29 - #3 (Ø 10 mm) stirrups plus 2 - #8 (Ø 25 mm) and 4 - #4 (Ø 13 mm) longitudinal rebars were embedded in this beam. The flexural beam has an estimated flexural strength according to ACI 318-14 (ACI 2014) of 340 kNm (251 kip-ft), corresponding to a total applied ultimate load of 357 kN (80.2 kip).

The second beam was designed to fail in shear-mode (Fig. 1b). This beam contained a total of 22 - #3 (Ø 10 mm) stirrups as well as 4 - #8 (Ø 25 mm) and 4 - #4 (Ø 13 mm) longitudinal rebars. To produce a region where inclined shear cracks would be generated at minor loading values without needing to force the beam to failure, the stirrups were spaced non-uniformly, with greater spacings on the right side and smaller spacings on the left side of the mid-span. According to ACI 318-14 (ACI 2014), the shear beam has an estimated shear strength of 259 kN (58.2 kips), which translates to a total applied ultimate load of 518 kN (116 kips). Cracking moment and corresponding total applied load are the same for both beams and estimated to be 68 kNm (50 kip-ft) and 68.9 kN (15.5 kip), respectively.

Recording system and data acquisition

AE signals were recorded during testing using a 16-channel high-speed transient recorder (Elsys TraNET FE, Elsys AG, Niederrohrdorf, Switzerland). AE signals were recorded for 1.2 ms at 10 MHz after a predetermined threshold was reached. 15 high-fidelity Glaser/NIST point-contact sensors (KRNBB-PC Sensor, KRN Services, Richland, WA, USA) were placed in the mid-span region (Fig. 1c) and the high-shear region (Fig. 1d), respectively, where most flexural and inclined shear cracks were anticipated to form, using specialized mounting fixtures by Mhamdi [7].

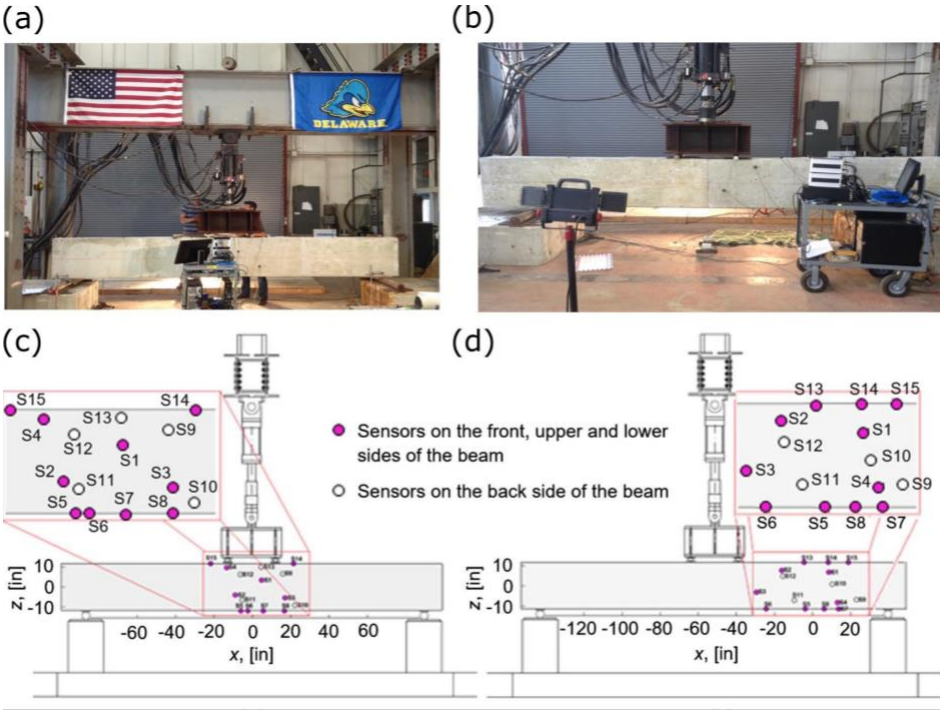

Figure 1. Experimental setup. The prepared reinforced concrete beams for flexural (**a**) and shear (**b**) crack tests. Locations of the Glaser/NIST sensors on the (**c**) flexure beam and (**d**) shear beam are shown in circles. Adapted from [7].

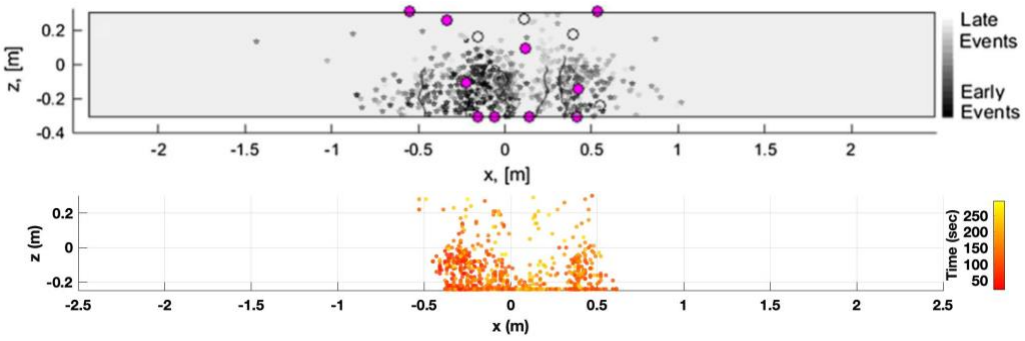

Figure 2. Sample comparison between 380 AE sources localized by manual processing [top, Figure from [7] and 1038 AE sources using SIMORGH (bottom) for the flexural beam loaded to 111 kN (25 kip). Purple circles show the sensor locations. Curved lines show the observed cracks at the end of the experiment.

Flexural beam test

The flexural beam was subjected to peak loads of 111 kN (25 kip), 133 kN (30 kip), and 156 kN (35 kip) at a rate of 22.2 kN/min (5 kip/min). After holding the load at the peak for several minutes to check the beam for cracks and record them, the beam was unloaded using the same rate to 2.22 kN (0.5 kip).

This made it possible to gather the most AE occurrences possible and accurately capture the cracking pattern. After each complete cycle, AE data were stored.

AEs from the first loading stage [111 kN (25 kip)] are shown in Figure 2. The localization errors are comparable to those selected by [7], with a standard deviation of localizations of 51 mm. At each loading stage, SIMORGH is able to locate over three times the number of AEs from the same dataset (Table I).

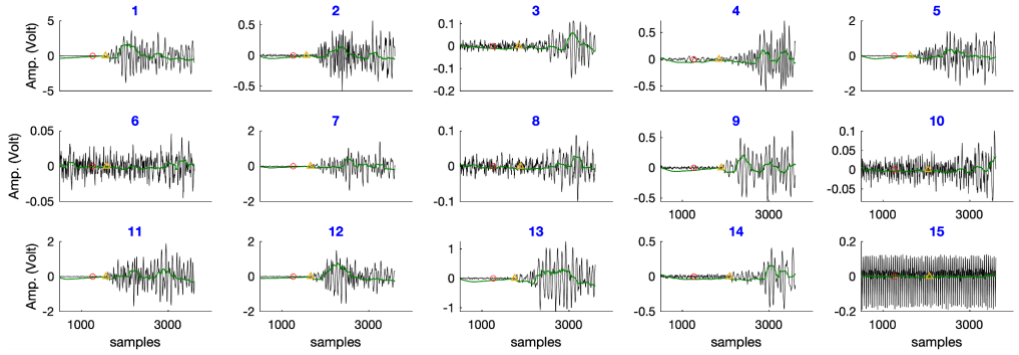

Figure 3. Example of localization of an AE on the flexure beam (Event No. 78 from the third loading stage). Each sub-figure shows the sensor's signals with their number labeled in blue. Green curves are modified envelopes. Orange triangle shows the final estimated P-wave arrival time obtained from the SIMORGH algorithm. Red circles denote the origin time

TABLE I. COMPARISON OF LOCATED AES FOR EACH LOAD CYCLE.

Test	Loading cycle(kips) min-max	Number of AEs ([7]) Total/selected	Number of AEs (SIMORGH) Total/selected	Relative Magnitude range (min/max)
Flexure beam	0-25	674/380	3159/1038	-3.9 / -1.3
	0-30	-	679/315	-3.76 / -1.6
	0-35	216/117	797/360	-3.6 / -1.7
Shear beam	0-25	40/20	436/171	-3.5 / -1.72
	0-35	57/29	673/367	-3.8 / -1.54
	0-45	40/24	502/273	-4.1 / -1.31
	0-55	116/53	1103/650	-3.9 / -1.26
	0-65	89/45	752/420	-3.9 / -1.45
	0-75	107/67	918/448	-3.8 / -1.26
	0-85	329/198	5145/1366	-4.1 / -1.33
	0-95	378/207	3068/1224	-3.7 / -1.4

The AE distribution pattern resembles that found by [7] and matches the observed cracks, supporting the accuracy of SIMORGH-localized AEs (Fig. 2).

Figure 3 shows the processed signal for sample event No. 78 from the third loading stage together with the estimated P-wave arrival times at the sensors and the origin time of the corresponding AE.

Shear beam test

The shear beam was loaded (using the same rate as the flexural beam) to 423 kN (95 kip) in increments of 44.5 kN (10 kip). The same holding and unloading procedure were used as for the flexural beam.

Similar to the flexural beam, we observe that SIMORGH can find over three times (up to 10 times!) as many AEs in the shear beam as compared to manual processing by [7] (Table I). The AE cloud provided by SIMORGH exhibits a similar pattern to that found by [7], and this pattern is consistent with the observed cracks, hence verifying SIMORGH's precise localization of AEs (Fig. 4).

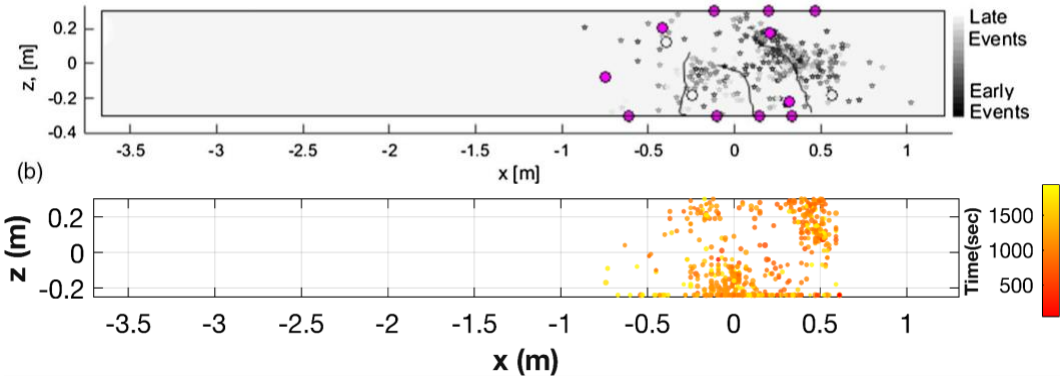

Figure 4. Sample comparison between 207 precisely located AE sources out of 378 localized AEs by manual processing [top, figure from [7] and 1224 precisely located AE sources out of 3068 AEs located using SIMORGH (bottom) for the concrete beam loaded to 423 kN (95 kip) shear force. Details are the same as Fig 2.

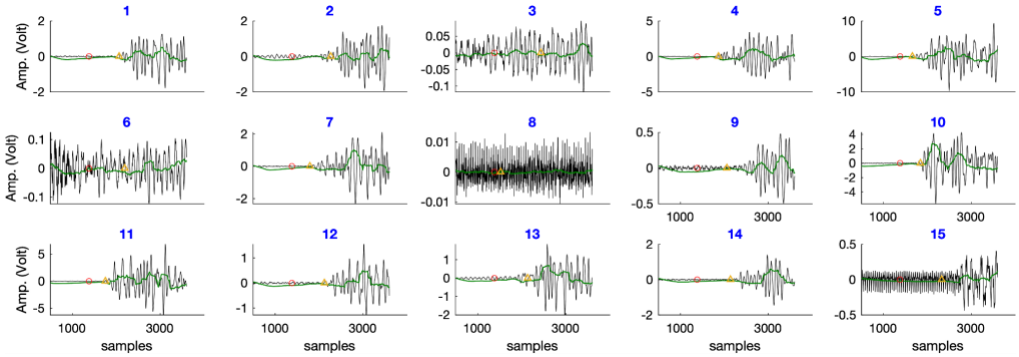

Figure 5. Example of localization of an AE on the Shear beam (Event No. 635 from the last loading stage, 423 kN). Details are the same as Fig. 3.

Figure 5 presents the localization information for event #635 from the latest loading stage. Even at stations with poor signals, the localized AE by Simorgh is able to predict the precise arrival time of the P-wave.

DISCUSSION

Correct signal processing before calculations, accurate implementation of the medium velocity model during calculations, and appropriate calculation method selection are necessary for accurate localization of AE sources. Consequently, manual localization of a single AE source typically requires 2 to 3 min, depending on the quantity of sensors (usually 8 to 20) and the quality of the signals needed to read the arrival times of P and S waves. SIMORGH, on the other hand, can localize a source in a fraction of a second, using every possible processor of the calculating unit. SIMORGH's parallelized method enables real-time fracture monitoring while maintaining excellent precision if sufficient computing power is available.

SIMORGH is capable of handling all potential medium complexities, from homogeneous, 1D layered, transversely isotropic, to fully 3D velocity models (using the Eikonal equation to identify the shortest ray path). Before selecting a solution, its smart algorithm evaluates each candidate path. The user can adjust over 40 defined hyper-parameters for the calculations. SIMORGH also offers comprehensive details on each AE source's location and mechanism.

Processing AE data corresponding to the two mentioned concrete beam tests and comparing with manual processing by [7] show that SIMORGH is able to perform the calculations about 1000 times faster and locate at least three times (up to 10 times) more AEs from the same dataset using similar precision criteria. This gives precise details about the location, geometry, and development of the fracture.

SIMORGH also offers other AE source features measurements such as frequency content of signals, magnitude, directivity, duration, and number of hits. Automatic moment tensor inversion, which provides details on the mechanism of fracturing material, is the key feature that has recently been added to this software package.

CONCLUSION

SIMORGH significantly reduces processing-localization costs and time with high precision, enabling real-time monitoring, which is currently not possible despite being essential in many fields, such as the need to locate growing fractures in geothermal energy, CO2 storage, oil and gas fields, dams, landslide-prone areas, plane bodies, railways, and other structures.

SIMORGH will allow the deployment of AE/MS surveillance arrays with confidence and reduced cost, leading to more of those arrays being routinely deployed and thus increasing public safety. To conclude, the developed software will have a significant impact on community security and safety, as well as environmental sustainability.

ACKNOWLEDGEMENT

This work is supported by the Swiss National Science Foundation (SNSF), Bridge Proof of Concept grant number: 40B1-0_214632.

REFERENCES

1. https://en.wikipedia.org/wiki/List_of_bridge_failures
2. Park, S., K.I. Kim, L. Xie, et al. 2020. "Observations and analyses of the first two hydraulic stimulations in the Pohang geothermal development site, South Korea" *Geothermics*, 88, 101905, https://doi.org/10.1016/j.geothermics.2020.101905.
3. Li, L., J. Tan, B. Schwarz, F. Staněk, N. Poiata, P. Shi, et al. 2020. "Recent advances and challenges of waveform-based seismic location methods at multiple scales" *Reviews of Geophysics*, 58, e2019RG000667.https://doi.org/10.1029/2019RG000667.
4. Van den Ende M.P.A., and J.P. Ampuero. 2020. "Automated seismic source characterization using deep graph neural networks" *Geophysical Research Letters*, 47(17), doi:10.1029/2020GL088690
5. Momeni, S., D. Liu, and B. Lecampion. 2021. "Combining active and passive acoustic methods to image hydraulic fracture growth in laboratory experiments". *Eurock21*, Turin, Italy, DOI:10.1088/1755-1315/833/1/012088.
6. Momeni, S., G. Lu, and B. Lecampion, 2021. "Automatic passive acoustic emission-microseismic monitoring using a parallel algorithm; A case study of a hydraulic-fracturing experiment" *SGM 19*, Geneva, Switzerland.
7. Mhamdi, L. 2015. "Seismology-based approaches for the quantitative acoustic emission monitoring of concrete structures." *Ph.D. dissertation, Univ. of Delaware*, Newark, DE.